Design and Prototype of Parallel, Wire-Actuated Robots with a Constraining Linkage

Geoff Mroz and Leila Notash
Department of Mechanical Engineering
Queen's University
Kingston, Ontario K7L 3N6
Canada

Abstract: Currently, wire-actuated robots are not used extensively in industry, but they are gaining more attention due to advantages they possess. Low weight, cost, and power consumption are features that make wire-controlled robots worth researching. This article investigates the designs of two different 4 degrees of freedom parallel, wire-actuated robots so that a prototype of one of these can be built. Stability of both designs is considered first to ensure that the robots are able to exert and withstand end effector forces in different positions throughout their respective workspaces. The stiffness and strength of the materials used in the designs is also investigated using finite element analysis.

Keywords: Design, Parallel Robots, Wire-Actuated, Stability, Strength, Stiffness

1. Introduction

Robotic manipulators, or mechanisms, are made up of links and joints. Link is the term given to the rigid bodies in the mechanism, and joint is the term given to the mechanical component that connects the links. Combining two links through the use of a joint produces a kinematic pair. Numerous links connected to one another is referred to as a kinematic chain or branch.

Serial manipulators consist of links that are connected in series. They are open loop mechanisms, which means that the mechanism uses a single kinematic chain or branch to connect the end effector to the base. The end effector is the name given to the tool that is attached to the end of the manipulator. In serial manipulators, it is necessary to actuate all of the joints in order to achieve control of the end effector.

Parallel manipulators employ multiple kinematic chains or branches to connect the end effector to the base and are therefore referred to as closed loop mechanisms. It is not necessary to actuate all of the joints in parallel manipulators, and often the joints at or close to the base are actuated to help reduce inertia. The best-known parallel manipulator is probably the Stewart platform [1]. This manipulator consists of six branches. Each branch is made up of an actuated prismatic joint that is connected to a base platform by using a universal joint, and connected to an

end effector platform by using a spherical joint. The Stewart platform is capable of motion in 6 degrees of freedom (DOF). Versions of this device are used today for such applications as machining, welding, and flight simulation.

Research in the field of parallel robots is important because of the advantages these machines can provide over serial robots. Currently, most of the robots used in industry have a serial configuration. Since parallel robots have multiple branches that connect the base platform to the end effector, this provides much higher stiffness, accuracy, speed, and load capacity than can be achieved with serial manipulators. However, serial manipulators generally have a larger workspace than parallel manipulators.

Wire-actuated robots are a special class of robots that can often provide advantages over the traditional robots used in industry. Machines that use hard actuators such as ball screws and pistons generally have higher accuracy and stiffness than wire-actuated devices, but for large-scale applications they become expensive. Large, wire-actuated robots can be built at fairly low cost, and can be made much lighter than machines that use hard actuators. Due to their low mass, which results in low weight and inertia, much lower power consumption can also be achieved. Low mass and low power consumption make wire-actuated robots very important for space applications.

To control an n DOF robot using only wires will require the use of a minimum of $n + 1$ wires [2, 3]. Accurately controlling the position of wire-actuated robots can be challenging, because all wires must be maintained in tension at all times. Also, most wire-controlled robots utilize a winch to wind and unwind the wire to control the length. To ensure that the wire is properly aligned with the winches as the robot changes position requires the use of guiding pulleys. For a spatial robot, these pulleys should be able to pivot so that the wires can follow the end effector as it moves [4]. This can lead to inaccuracies because as the pulley pivots, the actual length of the cable will change slightly.

A rigid central linkage is often necessary when designing wire-actuated robots if it is desired to constrain the mechanism to a specific motion. It is possible to design 6 DOF spatial, 3 DOF translational, and planar wire-controlled manipulators without a central linkage mechanism. However, when considering spatial manipulators with 4 or 5 DOF that require specific motion requirements, i.e., only allowing a rotation about a specific axis, some type of mechanical constraining device is usually necessary. The motion of the central linkage will dictate the motion of the end effector, and the main purpose of this linkage will be to eliminate any unwanted DOF.

A number of wire-actuated robots have been constructed for various applications. One of the early publications on wire-driven robots was by Landsberger and Sheridan [5]. This design is based on the Stewart platform, but

replaces the six rigid legs with wires. A telescopic spine is employed to ensure that the wires remain in tension at all times.

The National Institute of Standards and Technology (NIST) has designed and built numerous wire-actuated prototypes, called RoboCranes, based on the Stewart platform design. One of the first designs used a platform suspended from six wires, which were controlled by a single winch to provide 1 DOF [6]. The six wires provided more stability than a standard crane mechanism. A later design developed at NIST was the SPIDER [7]. This machine also incorporated a platform suspended by six wires. However, in this design each wire was controlled by a separate motor so that 6 DOF could be achieved. NIST also built a smaller prototype of a RoboCrane called the Mini-Tetra [8, 9], which is similar in function to the SPIDER. These NIST RoboCrane designs rely on gravity to completely constrain the motion of the end effector.

Numerous wire-actuated robots have been investigated by Kawamura's group, including a high-speed wire-controlled robot called FALCON7 [4]. This design incorporates seven wires that connect to an end effector and provide 6 DOF. The FALCON7 prototype was able to achieve very high speeds and accelerations. Another design developed by the same group was FALCON4 [10]. This device employs four wires and a mechanical constraint to achieve 3 DOF. The mechanical constraint helps reduce vibration in the mechanism. The same group also developed a large, wire-actuated robot that uses eight wires to achieve 5 DOF [11]. Although only $n + 1$ wires are needed to produce n DOF, the additional wires help to produce a wider motion range and reduce vibration.

Another machine, called CHARLOTTE VRR [12] has been used in training simulations at NASA's Johnson Space Centre. This robot uses eight wires to achieve 6 DOF. Motors located inside a central cube control the lengths of the wires. The wires exit this cube at each corner and attach to an external frame for support.

A wire-controlled robot that does not use pulleys and winches to control the lengths of the wires is WARP [13]. Instead, this design uses eight wires that are connected to the tips of motor-driven arms to provide 6 DOF.

The work presented in this article involves a comparison of the designs of two different 4 degrees of freedom (DOF) parallel robots. The designs have been developed based on specifications provided by MD Robotics, Ltd., which was interested in a parallel robot design that could be used for digging or soil sampling in outer space. At present, a prototype of one of the designs has been built. Although the prototype will not actually go into outer space, it will be used on earth for testing in the Queen's University Robotics Laboratory. Building a prototype is an important step in showing that the design is capable of functioning properly and performing well.

This article is divided into the following sections: Section 2 discusses the steps that should be followed when designing robots. Two case studies are given in Section 3, and include investigation of stability, strength, and stiffness, and wire attachment locations of both designs. The results from simulations are presented in Section 4, and Section 5 presents an analysis verification. Section 6 presents a discussion and conclusion.

2. Methodology

The designs of two different 4 DOF parallel, wire-actuated robots have been investigated. The first design has been presented and investigated in [14], and the second design is discussed in this article. The design process used follows six main steps:

1. *Robot Requirements*: This step involves investigating the possible applications of the robot. It is necessary to determine the motion, force, and accuracy requirements before deciding on the design type.

2. *Kinematics*: This involves ensuring that the designs achieve the motion and workspace requirements. Position analysis should be performed, and possibly velocity and acceleration analysis. If possible, a simple model should be simulated to verify the results.

3. *Stability*: This involves ensuring that the wire-controlled robot is able to exert/withstand end effector forces in all directions without losing tension in the wires and causing the end effector to move. The location of the wires is the most important factor in designing a stable robot. The initial wire selection can be based on the geometry of the robot, but it is very beneficial if the stability can be tested using a simulation or finite element analysis program.

4. *Strength and Stiffness*: It is important to ensure that the stresses developed do not cause failure of the components. Forces/stresses developed in the robot should be investigated for different positions and with various end effector loads so that the maximum values can be determined. The robot should be designed as stiff as is required to achieve the desired accuracy.

5. *Detailed Design Work*: This involves selecting materials, determining link and wire sizes, choosing actuators, and selecting joint sensors. It also involves using a 3D CAD program to design and assemble the links and joints. When the model is complete, it should be checked to ensure that there is no interference caused by the links, joints, or wires. As a final step, dimensioned drawings should be created so that all of the parts can be machined.

6. *Control System*: After the robot is assembled, the controller can be implemented. It is important that the control system ensures that tension is maintained in all wires as the robot moves.

The main focus of this article will be on steps 3 and 4, i.e., the stability, strength, and stiffness analysis of the robot.

3. Case Studies

The stability, strength, and stiffness of two different designs of 4 DOF robots were investigated. For both designs, three of the DOF are translations, and the remaining DOF is a pitch rotation. Each design utilizes a central linkage mechanism to constrain the robot to the desired motion and ensure that the end effector could only provide the required 4 DOF.

The designs, which are intended for digging or soil sampling in outer space, were developed based on specifications given by MD Robotics, Ltd. The general requirements for these robots are the following:

- Four degrees of freedom (DOF) – three translations, one pitch rotation.
- A cylindrical workspace with 2.20 m (86.6 in) radius and 2.00 m (78.7 in) height.
- A total mass under 8.00 kg (17.6 lbm).
- The ability to produce end effector forces of 23.0 N (5.17 lb) vertically and 16.0 N (3.60 lb) laterally.
- The ability to withstand shock loads of 15g at landing and launch.
- The capability to operate in outer space.
- Repeatability of 6.00 mm (0.236 in).
- Power draw below 20 W (0.027 hp) average, with 35 W (0.047 hp) peak draw allowable.

A ¼ scale prototype of one of the designs would be built.

3.1. First Design

The first design consists of a central linkage that is controlled by five wires. The central linkage is composed of two parallelogram mechanisms. The upper parallelogram consists of the base link, the right and left upper linkage beams, and the tie beam. The lower parallelogram mechanism consists of the medial beam, the right and left lower linkage beams, and the end effector raft. The central linkage incorporates 18 revolute joints to achieve the desired 4 DOF motion (Figure 1). The wires attach to points on the central linkage, and then pass over guiding pulleys and attach to winches that are actuated by DC servomotors. The motors are mounted to an overhead base. A global coordinate system is shown in Figure 1, and is used when referring to the first design. The lengths of the links and wire attachment points on the base used for testing the first design are listed in Table 1.

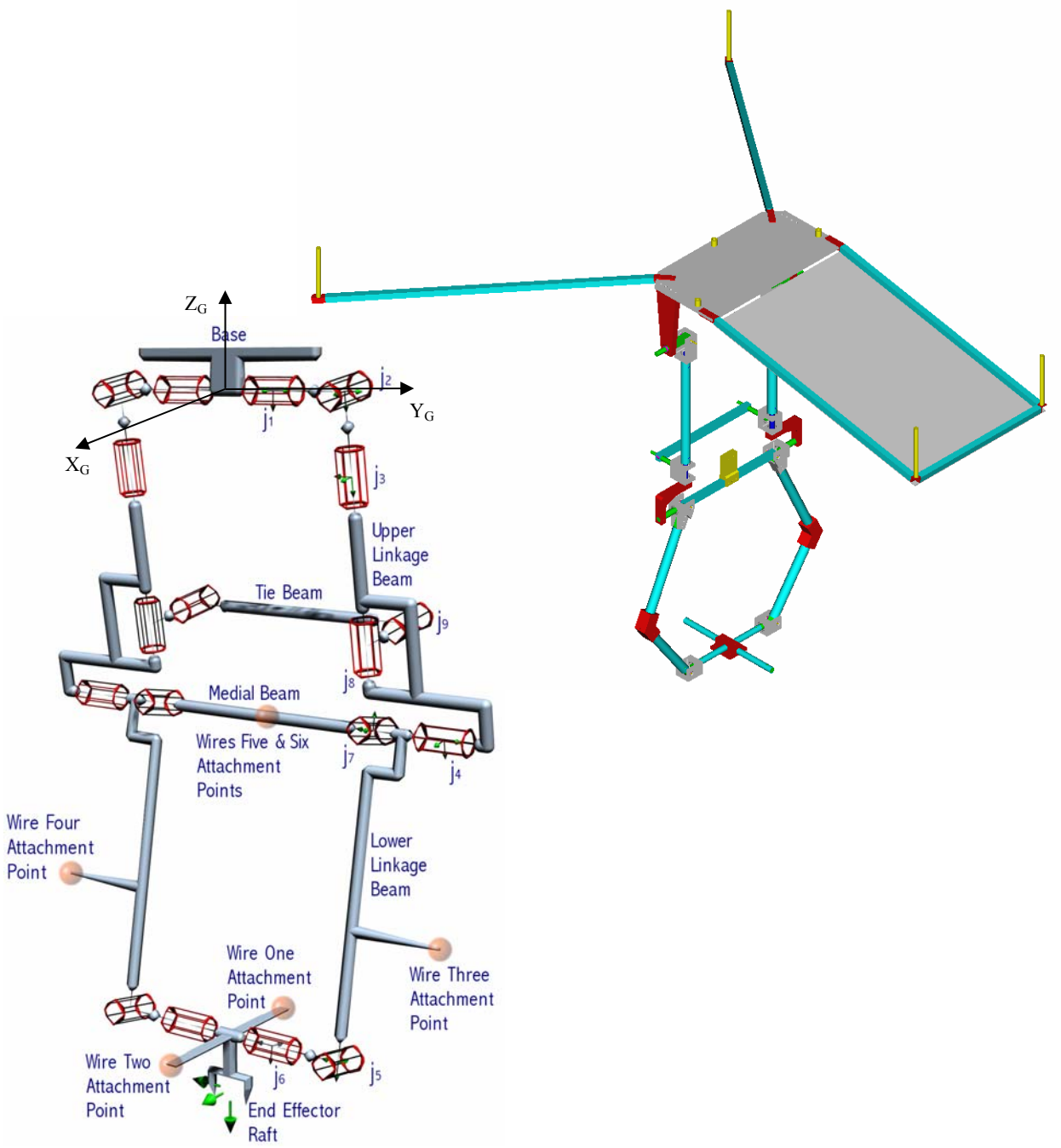

Figure 1: Central linkage configuration of first design (simplified link and joint diagram on left [15], and detailed drawing on right).

3.2. Second Design

The second design consists of a central linkage that could be controlled by a combination of motors for directly actuating some of the joints of the central linkage, and wires to control the remaining DOF of the robot. The central linkage incorporates a parallelogram mechanism, which is composed of the top shaft, the right and left top links, and

Table 1: Link lengths and wire locations for first design.

First Design	
Link Name	**Length (mm, in)**
Upper Linkage Beams	375 (14.76)
Lower Linkage Beams	375 (14.76)
Medial Beam	225 (8.86)
Medial Extension	50.8 (2.00)
Tie Beam	225 (8.86)
End Effector Raft	225 × 225 (8.86 × 8.86)
Wire Number	**Mounting Point on Base (mm, in)**
Wire 1	(100,0,100), (3.94, 0, 3.94)
Wire 2	(625, 0, 0), (24.6, 0, 0)
Wire 3	(-397.5, 660, 0), (-15.6, 26.0, 0)
Wire 4	(-397.5, -660, 0), (-15.6, -26.0, 0)
Wire 5	(400, 0, 37.5), (15.7, 0, 1.48)

the middle shaft. The middle shaft then joins to the bottom link, which in turn connects to the end effector plate. The central linkage incorporates 8 revolute joints to achieve the desired 4 DOF motion (Figure 2). As in the first design, the wires pass over guiding pulleys and attach to winches controlled by DC servomotors. Although not shown in the figure, two joints were used for joint j_1 in constructing the prototype to provide the necessary support for the top shaft. A global coordinate system is shown in Figure 2, and is used when referring to the second design. The lengths of the links and wire attachment points on the base used for testing the second design are listed in Table 2.

Different versions of the second design were tested, and a brief description of each is given below:

Version 1: For this design two of the joints of the central linkage, joints j_1 and j_{2A}, are actuated, and three wires are used to control the remaining 2 DOF of the end effector. Two of the wires are connected to two points on the end effector plate and the third wire is connected to a point on the middle extension. It was found that this hybrid method of control produced greater stability.

Version 2: This design consists of a completely passive central linkage that is controlled by five wires. Four of the wires mount to the end effector, and the fifth wire mounts to the middle extension.

Version 3: This design incorporates one motor attached to the overhead base that is used to control joint j_1, and four additional wires to control the remaining 3 DOF. Three of the wires are attached to the end effector, and the fourth wire is attached to the middle extension.

Version 4: This design utilizes four motors to directly actuate joints j_1, j_{2A}, j_3, and j_4. Wires are not incorporated.

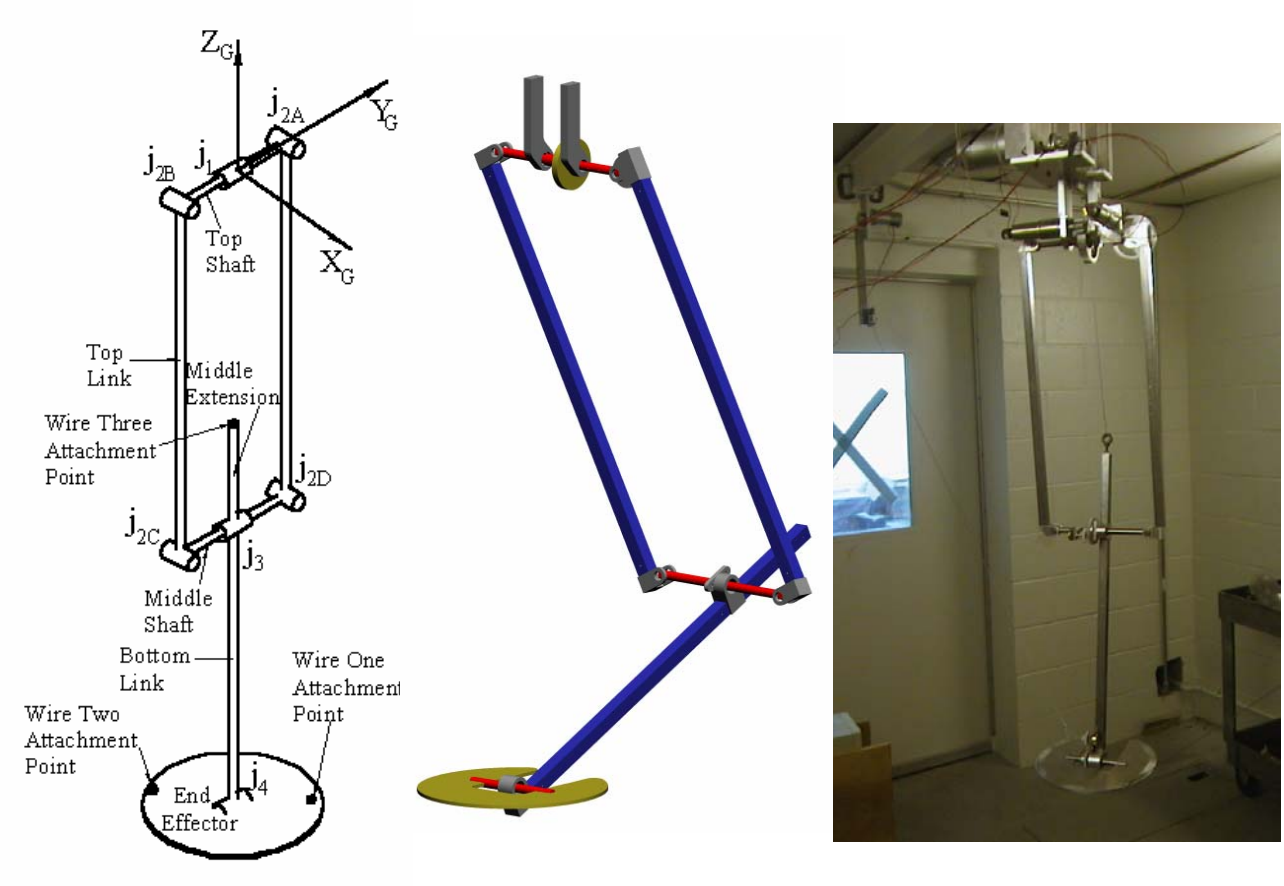

Figure 2: Central linkage configuration of second design (simplified link and joint diagram on left, detailed drawing in centre, and prototype on right).

Table 2: Link lengths and wire locations for second design.

Second Design	
Link Name	**Length (mm, in)**
Top Links	610 (24.0)
Bottom Link	483 (19.0)
Top Shaft	210 (8.25)
Middle Shaft	210 (8.25)
Middle Extension	178 (7.00)
End Effector Plate	254 Diameter (10 Diameter)
Wire Number	**Mounting Point on Base (mm, in)**
Wire 1	(889, 1143, 0), (35.0, 45.0, 0)
Wire 2	(-889, -1143, 0), (-35.0, -45.0, 0)
Wire 3	(-50.8, 0, 76.2), (-2.00, 0, 3.00)

3.3. Stability Testing

Stability testing involved applying forces to the end effector of the robot in different static positions to ensure that it would not lose tension in any of the wires and move. The simulation program visualNastran was used to test the robot, and the links and wires were modeled as rigid bodies.

3.4. Strength and Stiffness Testing

Strength and stiffness testing was performed in a similar manner to the stability testing. Forces were applied to the end effector of the robot in different static positions and the results were examined. The finite element analysis program ANSYS 5.7 was used, and the links and wires were modeled as linear elastic isotropic bodies. ANSYS 5.7 also proved useful for examining the stability of both designs, and provided more realistic results that visualNastran since it accounted for wire stretch and link deflection.

3.5. Wire Locations

Wire locations were originally chosen to ensure that the robot could exert and withstand end effector forces in any direction throughout the workspace. Since it is intended to use the robots for digging or soil sampling, it is desirable to avoid having the base points of the wires originate from a location below the end effector. However, if all wires originate from points above the end effector and are attached to the end effector, they will not be able to move the end effector in a downward direction without relying on gravity. Therefore, one wire was attached to an extension added to the middle beam of both the first and second design. As is shown in Figure 3, which relates to the second design, if tension is applied to wire three, the upper links will move forward in the positive X_G direction by rotating about joint j_1, and the lower links will tend to rotate about joint j_3. This will cause the end effector to move or exert forces down in the negative Z_G direction. This same situation also occurs for the first design.

For ensuring that the end effector can move within the full radius in the X_G and Y_G directions, it is necessary to examine what happens to the wires as the end effector moves to the edges of the workspace. For the second design, version 1, only wires one and two are attached to the end effector, which mainly control motion in the X_G and Z_G directions. Therefore, it is sufficient for these wires to attach to the base a distance from the origin in the X_G direction that is just greater than the sum of the workspace radius and the end effector radius.

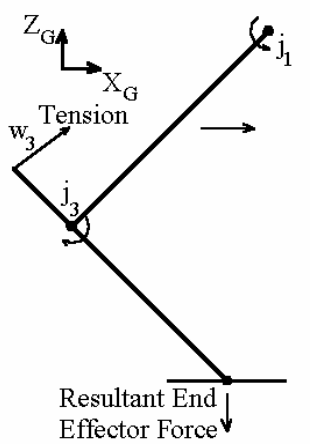

Figure 3: Side view of second design showing results of applying tension to wire three.

For a configuration that is actuated using five wires, such as the first design or version 2 of the second design, one wire should be attached to the middle extension, and the other four wires could be attached to the end effector plate. As is shown in Figure 4, if four wires are attached to the end effector plate, the base points of these wires must be a sufficient distance away from the origin so that at all end effector positions, at least one wire is able to pull the end effector into the desired position while the other wires remain in tension.

4. Results from Simulations and FEA

VisualNastran proved useful as an aid in selecting wire positions. Based on the tests, some modifications were made to the initial base point locations of the wires. It also showed that the first design became statically unstable when joint j_1 was rotated more than 60° and joint j_4 was rotated more than -120°, where a positive angle corresponds

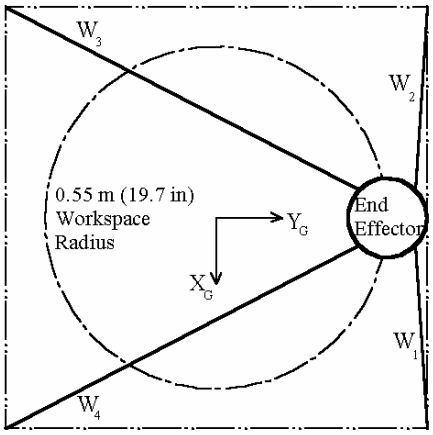

Figure 4: Wire locations chosen so that end effector can move to edge of workspace.

to a counter clockwise rotation about the Y_G-axis. However, some positions of the end effector that were stable in visualNastran were shown to be unstable when tested in ANSYS 5.7. This is due to modeling the links and wires as rigid bodies in visualNastran.

For the second design, the best results were obtained for version 1, the configuration with two motors and three wires; and version 4, the configuration in which motors are used to directly actuate the joints.

The second design, version 2 (with five wires), when tested in visualNastran, proved to be stable for all positions investigated. However, when tested in ANSYS 5.7, positions that had a large rotation about joint j_2 proved to be unstable. This was a result of modeling the links and wires as linear elastic isotropic bodies in ANSYS 5.7, which produced more realistic results than visualNastran. Although visualNastran is capable of modeling bodies as elastic members, this option was not used with this program. Modeling of the robot designs with elastic links and wires was performed using ANSYS 5.7.

Tables 3 and 4 list the names of the elements used in ANSYS 5.7 to model the links and wires for the first and second design, and the cross-sectional areas used for the links and wires. In these tables, *E* refers to the modulus of elasticity of the material, *v* refers to Poisson's ratio, and *O.D.* represents the outer diameter. Table 5 shows FEA results for the second design, version 1, and Table 6 shows FEA results for the second design, version 4. Several positions were tested [16] but due to space limitations only the results from positions P1 and P2 have been included in this article. In Tables 5 and 6 M1, M2, M3, and M4 are the motors that control joints j_1, j_{2A}, j_3, and j_4 respectively. Diagrams of positions P1 and P2 are shown in Figure 6.

Table 3: FEA parameters for first design using ANSYS.

Part	**Element Name (ANSYS)**	**Steel E = 200 GPa (30 000 ksi), v = 0.29**
Upper/lower links	PIPE16	19.05 mm (0.750 in) O.D., 0.889 mm (0.035 in) wall
End effector links	PIPE16	12.7 mm (0.500 in) O.D., 0.508 mm (0.020 in) wall
Middle/tie links	BEAM4	12.7 mm (0.500 in) square, 1.27 mm (0.050 in) wall
Wires	LINK10	2.38 mm (0.0938 in) diameter

Table 4: FEA parameters for second design using ANSYS.

Part	**Element Name (ANSYS)**	**Steel E = 200 GPa (30 000 ksi), v = 0.29**
Shafts	BEAM4	12.0 mm (0.472 in) diameter, solid
Upper/lower links	BEAM4	19.05 mm (0.750 in) square, 1.651 mm (0.065 in) wall
Wires	LINK10	3/32 diameter
		Aluminum E = 68.9 GPa (10 000 ksi), v = 0.35
End effector platform	SHELL63	4.76 mm (3/16 in) thick plate

For the second design, comparing the results shown in Table 5 for version 1, the hybrid design that is controlled with two motors and three wires, and the results shown in Table 6 for version 4, the design in which the joints are directly controlled by four motors, the following observations can be made:

- End effector displacements are higher for version 1, the hybrid model.
- Link stresses are higher for version 4, the fully joint actuated model.

These results are to be expected. The wires that are used in version 1 add additional support to the central linkage of the robot, and are therefore able to support some of the loading. The wires make the design more of a parallel structure, and help to lower the forces in the individual links. Version 4 is closer to a serial structure, and when a load is applied to the end effector, the links behave like cantilevered beams, which create higher forces and moments.

One might expect the displacement to be lower for version 1, the hybrid design. The deflections of the links are actually lower than that of version 4, since the forces and moments are lower. However, wire-controlled robots in general are not as stable as robots that have directly actuated joints. For wire-controlled robots with a constraining central linkage, there are often situations where the wires are not able to hold the central linkage in a completely stable configuration. Much of the end effector displacement for version 1 is due to rotation of the passive joints as opposed to deflection of the links and wires.

When examining the results of version 1 in position P2, it is seen that the end effector displacement is very high when a forward force (positive X_G-direction) is applied to the end effector. When examining the layout of the central linkage and wires shown in Figure 6 (b), it is seen that the distance between the attachment points of wire three to the base and central linkage is largest in the Y_G direction, and smallest in the X_G direction. Because of this, the moment about joint j_3 caused by an end effector force in the X_G direction will partly be balanced by the x-component of the force in wire three. Since the force in a wire is in the same direction as the wire, then due to the large component of length of wire three in the Y_G direction, the force component in this direction will need to be very high also. Therefore, the resultant force in wire three will be high. Furthermore, a small change in length of wire three will result in a large change in the X_G location of the attachment point of this wire on the central linkage, which causes the high displacement. To decrease this problem, the base location of wire three could be moved further forward in the X_G direction. However, this would cause interference with the central linkage.

5. Analysis Verification

To validate the results from ANSYS 5.7, a static analysis was performed for the second design, version 1, when in position P1. Joint angles for this position are given in Table 5. This was used to verify the torque on the motor of joint j_1 and the tension in wire three, which is attached to the middle extension. This analysis was performed without gravity, and with a force of 22.2 N (5 lb) applied to the end effector in the positive X_G direction. In this situation, there is no force in wire one, and the force in wire two is almost zero as well.

The free body diagrams used to calculate the reaction forces and moments are shown in Figure 5. Referring to Figure 5(c), the tension in wire three can be solved for by summing moments about j_3. The reaction forces at j_3 can then be solved for, and referring to Figure 5(b), the torque applied to the motor at joint j_1 can be found by summing moments about j_1. Using the free body diagram method, the tension in wire three is 60.5 N and the motor torque at joint j_1 is 9.71 N-m. The results from ANSYS are very close to the free body diagram method. From ANSYS, the tension in wire three is 60.5 N and the motor torque at joint j_1 is 9.72 N-m.

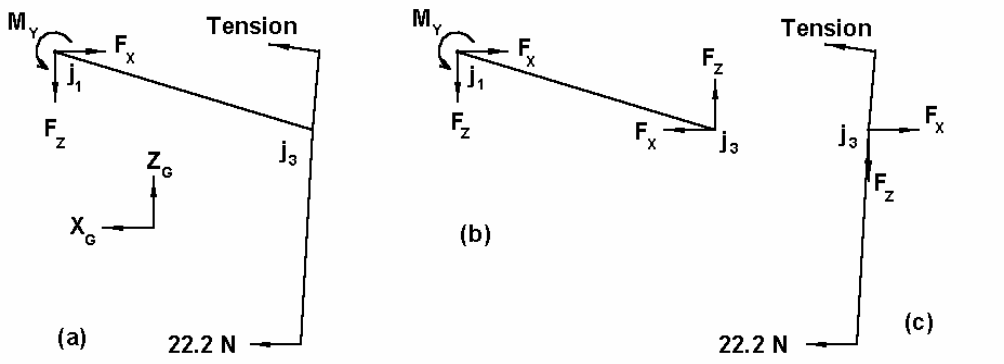

Figure 5: Free body diagrams of robot links for position P1 given in Table 5.

6. Discussion and Conclusions

The simulation of both designs indicated that the wire-actuated robots could experience large displacements and become unstable when a force is applied to the end effector, even when the links and wires are considered to be rigid bodies. To avoid or minimize this problem, it is extremely important to select the attachment points of the wires correctly. Much testing was performed with visualNastran and ANSYS 5.7 on the first and second designs so that acceptable wire locations could be selected.

Testing also showed that for wire-actuated robots with a central linkage, a small deflection in the links and wires could cause some of the wires to lose tension. This can result in large displacements of the manipulator by allowing

some of the passive joints in the central linkage to rotate. Therefore, in addition to selecting proper wire attachment locations, it is important to design the manipulator with sufficiently stiff links and wires. Adequate stiffness was ensured when designing the first and second designs to avoid these large displacements.

The unconstrained movement of the end effector is caused by the link deflection, wire stretch, and joint compliance, and is affected by the location of the wire attachment points. All of these factors contribute to finite displacement of the passive joints of the central linkage. Joint compliance, which is the play or slop associated with the joints, was not considered when modeling the designs. Also, any sagging associated with the wires was not considered. These issues could be investigated in the future.

Detailed design work has been completed for both designs, and a working prototype of the second design has been assembled and tested. A control system still needs to be developed for the robot. The second design was chosen for building a prototype due to the greater simplicity of the central linkage. Since good results were obtained for the second design, version 1, which is the configuration with two motors and three wires, and also for the second design, version 4, which is the configuration where the joints are controlled directly by motors, the prototype will allow for operation of both configurations.

Table 5: Stiffness and stress results from ANSYS 5.7 – Second design, version 1: two motors, three wires.

Position	Applied End Effector Force (N)	End Effector Displacement (mm)	Maximum Internal Moment (N-m)	Motor Torque (N-m)		Wire Force (N)			Maximum Stress (MPa)
				M1	M2	W1	W2	W3	
P1 Joint Angles (degrees) j1: 72 j2: 0 j3: -76 j4: 4	22.2 up [z] + Gravity	0.533	1.13 top of upper links	2.03	0.11	0.267	0	3.6	4.73 centre of middle shaft
	22.2 down [-z] + Gravity	6.78	9.72 near motor 2 & j_{2B}	19.2	0.68	24.0	18.2	37.4	28.6 shear in top shaft
	22.2 forward [x] + Gravity	10.5	1.24 bottom of extension	2.49	0	7.25	0	0	3.03 centre of middle shaft
	22.2 back [-x] + Gravity	1.83	2.03 near motor 2	3.73	0.45	34.7	23.1	0	9.03 lower shaft
	22.2 right [y] + Gravity	15.7	14.5 near motor 2	8.70	12.5	8.01	7.56	12.9	113 top shaft
	22.2 left [-y] + Gravity	12.3	13.3 near motor 2	9.61	12.3	12.5	6.67	22.7	7.81 centre of middle shaft
	22.2 up [z] (no Gravity)	3.07	6.44 top shaft, near motor 2	12.7	0.02	0.13	0	3.11	18.7 shear in top shaft
	22.2 forward [x] (no Gravity)	4.55	10.6 bottom of extension & top of lower link	9.72	0.1	0	0.044	60.5	28.3 centre of middle shaft
P2 Joint Angles (degrees) j1: 10 j2: 65 j3: -15 j4: 5	22.2 up [z] + Gravity	12.7	5.42 bottom of extension/ top shaft, near j_{2B}	0.0268	0.942	0	0.552	32.5	21.9 middle shaft
	22.2 down [-z] + Gravity	4.67	13.7 near motor 2 & j_1	0.791	13.0	30.2	49.4	12.5	90.5 top shaft near motor 2
	22.2 forward [x] + Gravity	108	40.3 bottom of extension	8.25	24.6	0	11.6	242	150 top shaft near motor 2
	22.2 back [-x] + Gravity	46.1	11.8 near motor 2	1.48	11.1	54.7	42.7	0	71.0 top shaft near motor 2
	22.2 right [y] + Gravity	6.02	3.05 near motor 2	0.0339	2.83	20.5	36.0	7.56	14.6 middle shaft
	22.2 left [-y] + Gravity	6.73	18.6 near motor 2 & j_1	1.02	17.4	16.0	24.5	24.5	98.7 top shaft near motor 2
	22.2 up [z] (no Gravity)	10.0	10.1 near motor 2 & j_1	0.565	9.83	0	0.0	33.4	56.5 top shaft near motor 2
	22.2 forward [x] (no Gravity)	113	45.7 bottom of extension	8.08	15.8	0	9.25	274	156 middle shaft

Table 6: Stiffness and stress results from ANSYS 5.7 – Second design, version 4: four motors.

Position	Applied End Effector Force (N)	End Effector Displacement (mm)	Maximum Internal Moment (N-m)	Motor Torque (N-m)				Maximum Stress (MPa)
				M1	M2	M3	M4	
P1 Joint Angles (degrees) j1: 72 j2: 0 j3: -76 j4: 4	22.2 up [z] + Gravity	0.991	1.81 top shaft & near j_{2A}, j_{2B}	3.62	0	0.452	0	5.33 shear top shaft
	22.2 down [-z] + Gravity	7.01	14.1 top shaft & near j_{2A}, j_{2B}	28.3	0	0.791	0	41.6 shear top shaft
	22.2 forward [x] + Gravity	10.8	15.3 top shaft & near j_{2A}, j_{2B}	30.6	0	10.5	0	45.1 shear top shaft
	22.2 back [-x] + Gravity	3.18	11.0 top of lower link	1.36	0	10.8	0	18.2 top of lower link
	22.2 right [y] + Gravity	8.03	17.4 near motor 2	15.9	13.6	0.113	0	123 top shaft near motor 2
	22.2 left [-y] + Gravity	8.15	15.6 near motor 2	15.9	13.6	0.113	0	119 top shaft near motor 2
	22.2 up [z] (no Gravity)	3.07	6.33 near motor 2 & j_{2B}	12.4	0	0.565	0	18.3 shear top shaft
	22.2 forward [x] (no Gravity)	6.88	10.7 top of lower link	14.7	0	10.7	0	21.6 shear top shaft
P2 Joint Angles (degrees) j1: 10 j2: 65 j3: -15 j4: 5	22.2 up [z] + Gravity	0.940	4.18 near motor 2	0.904	4.29	0.565	0	28.0 top shaft near motor 2
	22.2 down [-z] + Gravity	5.84	28.5 near motor 2	1.13	28.4	1.24	0	185 top shaft near motor 2
	22.2 forward [x] + Gravity	9.22	17.3 near motor 2	17.402	14.2	10.3	0	112 top shaft near motor 2
	22.2 back [-x] + Gravity	9.80	20.2 near motor 2	15.3	18.5	11.0	0	146 top shaft near motor 2
	22.2 right [y] + Gravity	2.69	12.7 near motor 2	1.02	10.5	0.339	0	70.2 top shaft near motor 2
	22.2 left [-y] + Gravity	5.44	22.9 near motor 2 & j_1	1.02	22.3	0.339	0	149 top shaft near motor 2
	22.2 up [z] (no Gravity)	2.59	12.1 near motor 2	0.113	12.1	0.90	0	78.9 top shaft near motor 2
	22.2 forward [x] (no Gravity)	8.66	10.7 near motor 2 & j_{2B}	16.4	2.15	10.7	0	45.1 top shaft right side

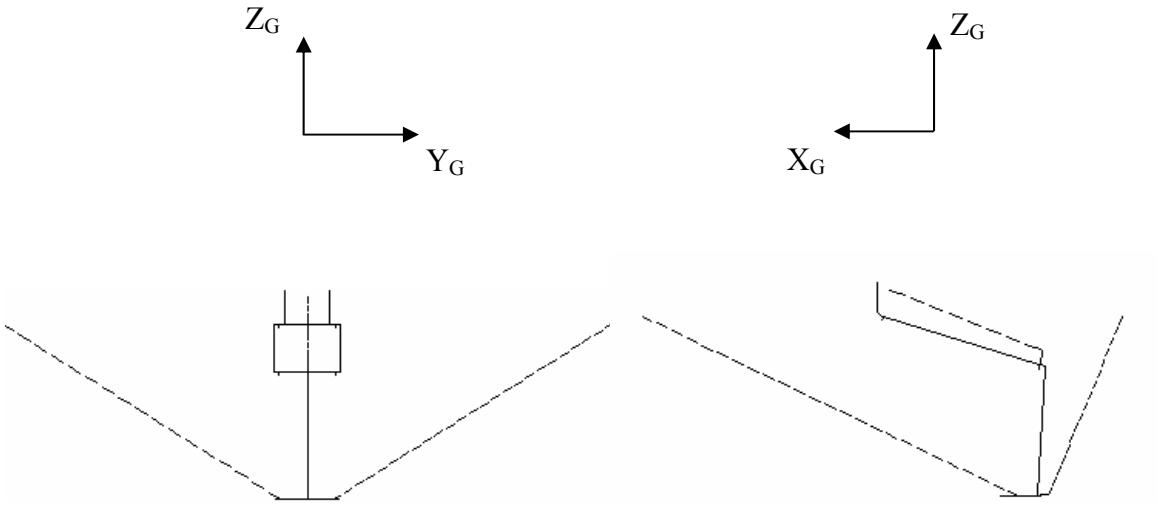

(a) Position P1

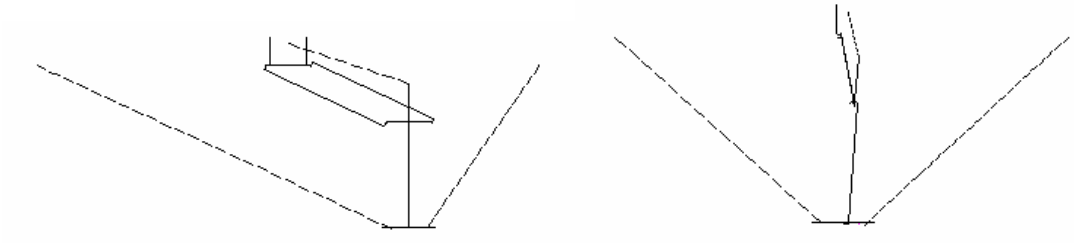

(b) Position P2

Figure 6: Front and right side views of two configurations tested for second design. Dashed lines represent wires.

References

1. Stewart, D., A Platform with Six Degrees of Freedom, Proc Instn Mech Engrs, Vol. 180, No. 15, 1966, pp. 371-378.
2. Kawamura, S., and Ito, K., A New Type of Master Robot for Teleoperation Using A Radial Wire Drive System, Proc. of IEEE/RSJ Int. Conf. on Intelligent Robots and Systems, Vol. 1, 1993, pp. 55-60.
3. Ming, A., and Higuchi, T., Study on Multiple Degree-of-Freedom Positioning Mechanism Using Wires (Part 1) – Concept, Design, and Control, Int. J. Japan Society for Precision Engineering, Vol. 28, No. 2, 1994, pp. 131-138.
4. Kawamura, S., Kino, H., and Won, C., High Speed Manipulation by Using Parallel Wire-Driven Robots, Robotica, Vol. 18, 2000, pp. 13-21.

5. Landsberger, S.E., and Sheridan, T.B., A Minimal, Minimal Linkage: The Tension-Compression Parallel Link Manipulator, Robotics, Mechatronics and Manufacturing Systems, 1993, pp. 81-88.
6. Dagalakis, N., Albus, J., Wang, B., Unger, J., Lee, J., Stiffness Study of a Parallel Link Robot Crane For Shipbuilding Applications, Proc. of Seventh Int. Conference on Offshore Mechanics and Arctic Engineering, Houston, Texas, February 7-12, 1988, Vol. 111, August 1989, pp. 183-193.
7. Albus, J., Bostelman, R., and Dagalakis, N., The NIST SPIDER, A Robot Crane, J. Research of NIST, Vol. 7, No. 3, 1992, pp. 373-385.
8. Bostelman, R., Jacoff, A., Proctor, F., Kramer, T., and Wavering, A., Cable-Based Reconfigurable Machines for Large Scale Manufacturing, Proc. of Japan-USA Symp. on Flexible Automation: Int. Conf. New Technological Innovation for the 21st Century, Ann Arbor, 2000.
9. Bostelman, R., Jacoff, A., Proctor, F., Weiss, B., Sagar, R., Mini Tetra Mechanical Designs and System Description, Technical Report, National Institute of Standards and Technology, Gaithersburg, Maryland, January 2001.
10. Choe, W., Kino, H., Katsuta, K., Kawamura, S., A Design of Parallel Wire Driven Robots for Ultrahigh Speed Motion Based on Stiffness Analysis, Proc. of Japan USA Symposium on Flexible Automation, 1996, pp. 159-166.
11. Kino, H., Miyazono, H., Choe, W., Kawamura, S., Realization of Large Workspace Using Parallel Wire Drive Robots, Proc. of 2nd Asian Control Conference, Seoul, Korea, July 22-25, 1997, pp. 591-594.
12. Eichstadt, F., Campbell, P., and Haskins, T., Tendon Suspended Robots: Virtual Reality and Terrestrial Applications, Proc. of 25th Int. Conf. on Environmental Systems, San Diego, 1995, pp. 1-6.
13. Maeda, K., Tadokoro, S., Takamori, T., Hiller, M., Verhoeven, R., On Design of a Redundant Wire-Driven Parallel Robot WARP Manipulator, Proc. of IEEE Int. Conference on Robotics and Automation, Detroit, Michigan, May 1999, pp. 895-900.
14. Kossowski, C., and Notash, L., CAT4 (Cable Actuated Truss - 4 Degrees of Freedom): A Novel 4 DOF Cable Actuated Parallel Manipulator, J. Robotic Systems, Vol. 19, No. 12, 2002, pp. 605-615.
15. Kossowski, C., A Novel Wire Driven Parallel Robot: Design, Analysis and Simulation of the CAT4, M.Sc. Thesis, Department of Mechanical Engineering, Queen's University, 2001.
16. Mroz, G., Design and Prototype of a Parallel, Wire-Actuated Robot, M.Sc. Thesis, Department of Mechanical Engineering, Queen's University, 2003.